
Algorithmic Capture, Computational Complexity, and Inductive Bias of Infinite Transformers

Orit Davidovich¹ Zohar Ringel²

Abstract

We formally define *Algorithmic Capture* (i.e., “grokking” an algorithm) as the ability of a neural network to generalize to arbitrary problem sizes (T) with controllable error and minimal sample adaptation, distinguishing true algorithmic learning from statistical interpolation. By analyzing infinite-width transformers in both the lazy and rich regimes, we derive upper bounds on the inference-time computational complexity of the functions these networks can learn. We show that despite their universal expressivity, transformers possess an inductive bias towards low-complexity algorithms within the Efficient Polynomial Time Heuristic Scheme (EPTHS) class. This bias effectively prevents them from capturing higher-complexity algorithms, while allowing success on simpler tasks like search, copy, and sort.

1. Introduction

A central yet unresolved question in the study of Large Language Models (LLMs) is the extent to which the procedures they execute involve genuine “understanding” or merely exploit statistical correlations to interpolate a domain. Empirical work has often highlighted the fragility of this understanding; for instance, the GSM-Symbolic benchmark (Mirzadeh et al., 2025) (see also (Anil et al., 2022)) shows that performance on mathematical reasoning can degrade significantly when symbolic templates are altered, suggesting a reliance on pattern matching rather than robust algorithmic execution. Still, the loose and somewhat philosophical nature of these terms hinders rigorous progress.

One realm where statistical learning can be clearly discerned from proper learning is *algorithmic learning*. Here, generalization to arbitrarily large problem instance sizes (n) is

¹IBM Research, Haifa, Israel. ²Racah Institute of Physics, Hebrew University, Jerusalem, Israel. Correspondence to: Zohar Ringel <zohar.ringel@mail.huji.ac.il>.

an inherent requirement. Such strong out-of-distribution (OOD) settings make statistical correlation and simple interpolation far less effective (Xu et al., 2020). Furthermore, the algorithmic setting provides a reliable ground truth regarding worst-case, average-case, and heuristic complexity. These theoretical bounds can be contrasted with the computation required for model inference, allowing us to refute the possibility that a network “grokked” (Power et al., 2022) an algorithm without needing to interpret its inner workings. Finally, transformers – the core technology behind LLMs – can operate on variable sequence lengths, naturally lending themselves to this scalable setting once we align problem size with context length ($T = n$).

In this work, we analyze whether the inductive biases of transformers inhibit or promote algorithmic understanding. As such research is in its early stages, this work sets aside the potential, yet not at all obvious (Dong et al., 2021; Gromov et al., 2025), computational complexity benefits of scaling depth and scratchpads and focuses on the complexity of single-token predictions. To enable arbitrarily complex functions and remove trivial computational bottlenecks associated with finite-depth, we consider infinitely over-parameterized networks in both the “lazy” and “rich” regimes.

Our key contributions are:

- 1. Formal Definition of Algorithmic Learning:** We provide a verifiable definition of what it means for a neural network to *capture an algorithm*. This definition, stated formally below, involves an input measure that is scalable across problem sizes ($\mu_{X,T}$), an arbitrary but finite sample budget $P_0(\delta)$ for obtaining the correct problem instance output with probability $(1 - \delta)$ on instances up to size T_0 , and a small logarithmic budget ($O(\log(T/T_0))$) for fine-tuning on larger instance sizes ($T > T_0$). This logarithmic allowance is provided solely to correct for architectural non-idealities, such as attention dilution and positional encoding drift, rather than to learn the task logic itself.
- 2. Examples of Captured and Non-Captured Algorithms:** We show a transformer that captures the induction head search-like algorithm and sorting. Con-

Regime	Evaluation	Inference Complexity	Evaluation Error	EPTHS
NNGP/NTK	Kernel estimate (MC)	$O(PN_{\text{MC}}T^3)$	$\sqrt{P/N_{\text{MC}}}$	$O(T^{3+\epsilon})$
	Forward-pass (large but finite-width)	$O(NT^2)$	P^γ/N	$O(T^{2+\epsilon})$
Rich Mean-Field Scaling	Forward-pass (large but finite-width)	$O(NT^2)$	P^γ/N	$O(T^{2+\epsilon})$

Table 1. Summary of infinite-width transformer inference-time complexity dependent on the context length T ; the number of training data points P ; the number of Monte Carlo samples N_{MC} ; the width of the estimating finite transformer N ; a T -independent constant $\gamma > 0$; and one can take any $\epsilon > 0$. For the heuristic complexity class EPTHS, see Sec. 3.

versely, we show several transformers, including very deep ones, that fail to capture the source-target shortest path problem (SPP) problem and Max Flow / Minimal Cut (MinCut) problem.¹

- Upper Complexity Bounds:** We show that, while performing a forward-pass on a finite-depth, infinite-width transformer requires infinite compute, the predictor can be evaluated using only $O(PdT^3)$ floating-point operations (FLOPs) on a serial machine (with P data samples of d input dimension). As a corollary, we prove that an infinite-width transformer, despite being expressive enough to represent arbitrarily complex functions, cannot capture an algorithm of heuristic complexity beyond $O(T^{3+\epsilon})$. Further making the reasonable assumption that transformers converge to their rich or lazy infinite-width limits when the number of heads and internal dimensions scale as P^γ , for some architecture-dependent exponent γ independent of T , we show that both lazy and rich transformer networks cannot capture an algorithm of heuristic complexity beyond $O(T^{2+\epsilon})$. This suggests that, while feature learning can have drastic sample complexity effects (Bietti et al., 2022; Wei et al., 2019; Ghorbani et al., 2020), it does not have similar inference complexity effects. Our results are summarized in Table 1.

Finally, we comment that our main purpose here is to present a framework in which computational complexity theory, OOD inductive bias of transformers, and shortcut learning can be sharply defined and contrasted. In particular, further refinement to the inductive bias we find towards lower complexity functions is needed to explain some of our numerical results, in particular those on the SPP.

2. Related Work

Our work intersects with several active areas of deep learning and complexity theory.

¹We comment that for our choice of critical graphs, we obtain sparse connectivity, implying that SPP can be solved in $O(T)$ compute.

Grokking and Algorithmic Reasoning: The phenomenon of “grokking” – where generalization emerges long after overfitting – has been widely observed in math tasks (Power et al., 2022; Barak et al., 2022; Nanda et al., 2023). However, these tasks have $O(\log(n))$, $O(1)$ computational complexity and, more crucially, experiments were carried out on specific instance sizes, rendering computational complexity ill-defined.

Kolmogorov and Sample Complexity. Prior work in algorithmic information theory suggests that neural networks are strongly biased towards functions with low Kolmogorov complexity (Valle-Pérez et al., 2019; Dingle et al., 2018). This is a different notion of complexity, which, for functions representing an algorithm, does not scale with input size. In addition, various works (Bietti et al., 2022; Ghorbani et al., 2020; Wei et al., 2019) studied the effect of feature learning on sample complexity. However, functions which are hard to learn are not necessarily hard to compute (e.g. k -sparse parity).

Worst-case Expressivity / Circuit Complexity. A complementary line of work studies transformers as constant-depth threshold circuits, placing them in TC^0 (Merrill et al., 2022; Chiang et al., 2023). More recently, Chen et al. (2024) established an unconditional lower bound for multi-layer decoder-only transformers. In contrast, our perspective is “softer”. We analyze average-case behavior and learnability via infinite-width limits (NNGP/NTK), where success is approximate and often stated in high probability, and where complexity is tied to inference cost / kernel evaluation rather than to exact worst-case computation. In the limit, we have universal expressivity, and thus focus on inductive bias, whereas the aforementioned literature addresses limits to expressivity.

Algorithmic Alignment and Graph Neural Networks (GNN). Prior work (Xu et al., 2019; 2020; Veličković et al., 2020) has argued that successful algorithmic extrapolation requires the network’s architecture to be structurally isomorphic to the target algorithm’s dynamic programming steps (see also Abbe et al. (2024)). This is consistent with our numerical findings for induction heads and sorting, which

are natural for a transformer (Weiss et al., 2021). However, these works primarily focus on bounds for in-distribution sample complexity and provide strong empirical evidence that algorithmic alignment is sufficient for good OOD generalization (see also Zhou et al. (2024)). They also work with strong step-by-step supervision. In contrast, our work offers a sharp definition for algorithmic capture with standard supervision, links it directly to inference-time complexity, and derives a formal “unlearnability” result, proving that, despite our networks’ universal expressivity, algorithms exceeding certain (heuristic) complexity cannot be learned regardless of alignment. Finally, we note that preliminary experiments we carried out on GNNs showed good generalization in-distribution but failed to capture the algorithm under standard supervised training.

3. Setting and Definitions

We consider supervised learning of optimization algorithms with discrete outputs having a minimal spacing of Δ , namely, the distance between any two possible outputs $\geq \Delta$. We assume a family of probability measures $\{\mu_{X,T}\}_{T \geq 1}$ on the instance space at size T , from which we can efficiently sample; when appropriate (e.g., for graph problems), $\mu_{X,T}$ is chosen in the critical regime (e.g., large clusters). By convention, we use $X \in \mathbb{R}^{T \times d}$ to denote an input data-point and x_a , $a \in [T]$, to denote its embedded tokens. Then T denotes the input sequence length and d the input dimension.

We say that a transformer can *capture an algorithm* A under $\mu_{X,T}$ at sufficiently small accuracy $\delta > 0$ if there exist $T_0 = T_0(\delta)$, $C = C(\delta)$, and $P_0 = P_0(\delta)$ such that the transformer will return $A(X)$ (up to $\Delta/3$) for every $T \geq T_0$ with probability at least $1 - \delta$ over a test draw $X \sim \mu_{X,T}$ when trained using the following two-stage protocol: (1) initial training on P_0 samples from $\mu_{X,1}, \dots, \mu_{X,T_0}$; (2) secondary fine-tuning using $C \log(T/T_0)$ additional samples from $\mu_{X,1}, \dots, \mu_{X,T}$. Alternatively, we allow M separate fine-tuning stages with $T_0 < T_1 < T_2 \dots < T_M = T$ with $C \log(T_m/T_{m-1})$ additional data-points sampled from $\mu_{X,1}, \dots, \mu_{X,T_m}$. The fine-tuning stage(s) are necessary to avoid trivial pitfalls, such as attention dilution. In a Bayesian context, we simply allow P_0 datapoints from $\mu_{X,1}, \dots, \mu_{X,T_0}$ and additional $C \log(T/T_0)$ points from $\mu_{X,1}, \dots, \mu_{X,T}$. Fig. 1 demonstrates two instances of algorithmic capture and two instances of its failure.

We view such trained transformers through the prism of heuristic complexity classes and distributional problems (Bogdanov & Trevisan, 2006). An algorithm A is an *efficient polynomial-time heuristic scheme* (EPTHS) of complexity $O(T^k)$ for a distributional task under $\mu_{X,T}$ if for every $\delta \in (0, 1)$ there exists an implementation A_δ such that $A_\delta(X)$ returns a $\Delta/3$ -accurate value for the algorithm’s task in time $O(\eta(1/\delta)T^k)$ with probability at least $1 - \delta$ over

$X \sim \mu_{X,T}$.² In principle, η is allowed to be exponential (or worse) in $1/\delta$. Average-case polynomial-time complexity of an algorithmic task establishes an upper bound for EPTHS: if an algorithm A returns a correct value $A(X)$ for every $X \sim \mu_{X,T}$ in time $t(X)$ and if $\mathbb{E}_{X \sim \mu_{X,T}}[t(X)] = O(T^k)$, then A establishes an EPTHS of complexity $O(T^k)$ for the distributional task under $\mu_{X,T}$. By Markov’s inequality

$$\Pr_{X \sim \mu_{X,T}} [t(X) \geq \mathbb{E}_{X \sim \mu_{X,T}}[t(X)]/\delta] \leq \delta.$$

Then, as a δ implementation, A_δ , run A on an instance X for up to $O(\mathbb{E}_{X \sim \mu_{X,T}}[t(X)]/\delta)$ steps. If A finished within the allotted step budget, provide its output, otherwise, output a random value for the task. By construction, $\Pr_{X \sim \mu_{X,T}} [|A_\delta(X) - A(X)| = 0] > 1 - \delta$ in time $O(T^k/\delta)$ where $A(X)$ is correct.

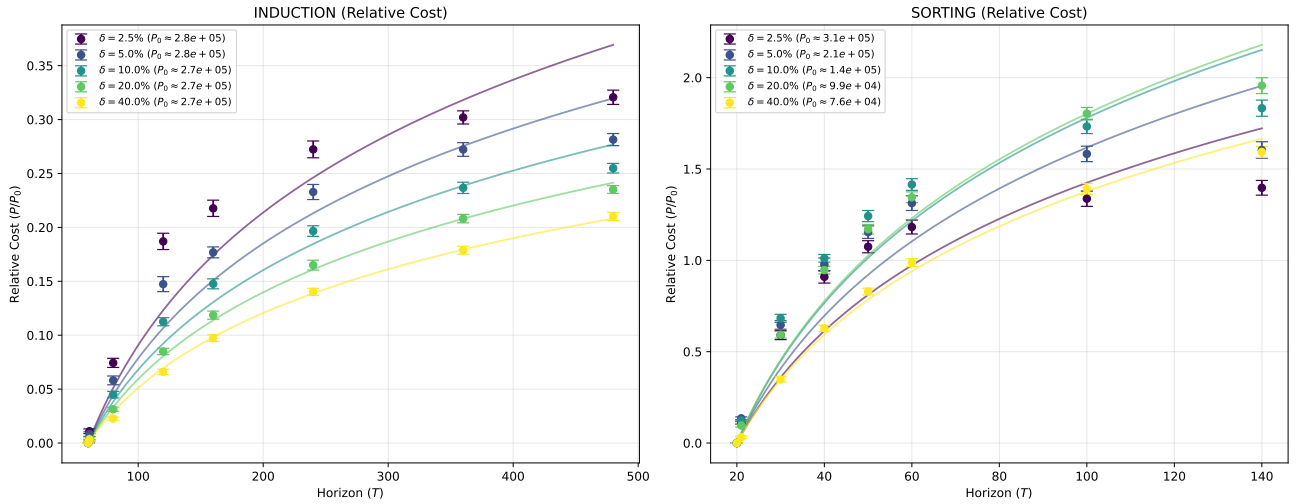
Below, we will argue that, if a transformer captured an algorithm, its kernel predictor is an EPTHS w.r.t. the algorithm’s task with $k = 3 + \epsilon$, and down to $k = 2 + \epsilon$, depending on assumptions, for any $\epsilon > 0$. Consequently, if the inference-time heuristic computational complexity of the transformer scales weaker than the target algorithm heuristic complexity, the transformer will not be able to capture that algorithm. Part of this work is dedicated to bounding this inference-time compute for transformers trained using the above two-stage protocol.

Architecture-wise, we focus on decoder-only transformers with softmax self-attention and no causal masking. Our inputs $X \in \mathbb{R}^{T \times d}$ will represent problem instances of size T , e.g., computing the length of the shortest path from a specific source to a specific target node. For problems in which all sequence indices in X are interchangeable, apart from $O(1)$ special tokens (e.g. those representing source and target nodes in graph problems), we encode such large symmetry using positional encoding that only distinguishes between special tokens and the rest. For instance, for the SPP, the actual input to the transformer will be \tilde{X} , given by concatenating one-dimensional vectors to rows of the SPP instance representation X : $[1]$ for $a = 1, T$ (as they play symmetric roles) and $[0]$ otherwise.

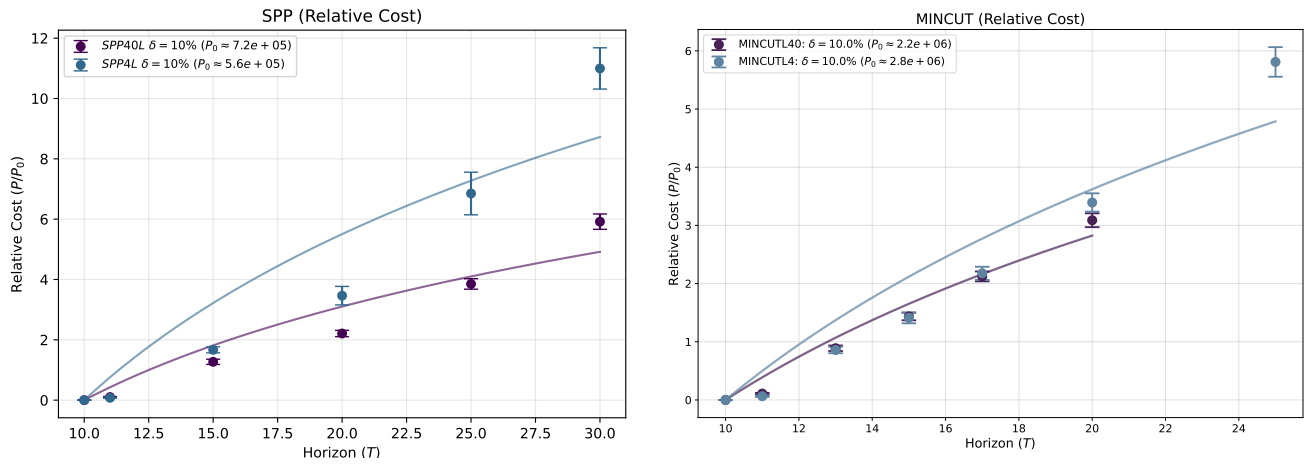
4. Low Complexity Bias of Lazy Learning

Finite networks have inference-time complexity bounded by the number of FLOPs needed for their forward-pass, which, for transformers, scales as T^2 (see App. A.2), and, thus, finite transformers cannot express functions that require more than $O(T^2)$ computational steps to evaluate. Infinitely-wide networks, however, are universal approximators and, thus, expressivity-wise, have unbounded complexity. Still,

²By analogy to an efficient polynomial-time approximation scheme (EPTAS), but swapping guarantees: EPTAS gives $(1 + \epsilon)$ -solutions for all inputs while EPTHS gives exact solutions for most inputs (w.h.p. over $\mu_{X,T}$).



(a) Induction and Sorting Tasks



(b) SPP Shallow vs Deep

(c) Mincut Shallow vs Deep

Figure 1. Empirical Verification of Algorithmic Capture. We train models on problem instances of size T_0 reaching accuracy δ after seeing $P_0(\delta)$ data points. We then fine-tune these models on larger instance sizes ($T > T_0$), re-achieving δ -accuracy after seeing P extra datapoints. Dots are average empirical values based on 20-40 transformer networks, and solid lines are best fits to $C \log(T/T_0)$ meant to guide the eye. For induction and sorting, P appears bounded by a logarithmic growth, suggesting algorithmic capture. However, for Shortest Path and Minimal Cut, both very deep (40 layers) and standard (4 layers) architectures exhibit a superlinear growth. For further experimental details see App. C.

their inductive biases may very well bias them towards low computational complexity solutions. To this end, we seek to analyze and upper bound the inference-time complexity of a trained transformer in the extreme over-parameterized limit (Hron et al., 2020).

4.1. The Infinite-width Limit

In a suitable limit of infinite width, deep neural networks initialized with standard scaling evolve linearly in their parameters (Hron et al., 2020; Jacot et al., 2018). The network predictor $f(X)$ converges to a kernel predictor defined by the NTK. The kernel predictor takes the form of a weighted sum over the training dataset $\{X_\nu\}_{\nu=1}^P$

$$f_K(X_*) = \sum_{\nu=1}^P \alpha_\nu K(X_*, X_\nu). \quad (1)$$

Thus, instead of performing a forward-pass through the network, we consider the computation complexity of evaluating Eq. (1): it is the product of the circuit size P and the architectural cost of evaluating $K(\cdot, \cdot)$.³ Accordingly, we analyze the number of FLOPs required to compute the kernel entries. Here, the kernel $K(X_1, X_2)$ depends only on the inner product of the inputs.

We note that the two-step learning protocol used in our experiments has a corresponding NTK formulation (Bennani et al., 2020), where the final predictor is the first-step predictor plus the NTK predictor associated with second-step acting on the errors made by the first-step predictor. Finally, we assume $|\alpha_\nu|$ are upper bounded by a P -independent constant, as would be the typical case. We note that our proof below also accommodates an $O(\sqrt{P})$ bound for $|\alpha_\nu|$, which is the worst-case for finite ridge.⁴

4.2. The Fully-connected Network

As a warm-up, consider a fully-connected network (FCN) acting on a flattened version of X . The complexity of evaluating the FCN Neural Network Gaussian Process (NNGP) kernel for a sequence of length T is dominated by the dot product scaling as $O(Td)$. Crucially, NNGP kernel recursions are element-wise on the Gram matrix, involving no mixing across sequence indices. Consequently, depth (L) only adds an additive $+L$ term to the inference-time computational complexity. Due to various fixed-points which appear in these recursions, the infinite-depth limit is also likely to be of finite computational complexity (Schoenholz et al., 2017). Next, we turn to the more interesting case of

³As we are evaluating inference-time complexity, matrix inversion in $\alpha = (K + \kappa I_P)^{-1} \mathbf{y}$ is not incorporated. We consider it to be a part of training complexity.

⁴By scaling N_{MC} , defined below, by an additional factor of \sqrt{P} .

the transformer, where sequence indices interact in Cho & Saul (2009) recursion.

4.3. Kernel Propagation

We now turn to transformer networks (see App. A.1 for a detailed setup) whose infinite width / attention limit was analyzed by Hron et al. (2020). The sufficient statistic (at infinite width) describing the transformer block’s state in the NNGP limit is the **token-to-token covariance matrix** $\Sigma'(X_1, X_2) \in \mathbb{R}^{T \times T}$ between inputs X_1, X_2 ,

$$\Sigma'_{ab}(X_1, X_2) = \lim_{d_{\text{model}} \rightarrow \infty} \frac{1}{d_{\text{model}}} \mathbb{E} [z'_a(X_1)^\top z'_b(X_2)], \quad (2)$$

where $z'_a(X)$ are the outputs of the MLP layer of the previous transformer block, which are multivariate Gaussian at infinity. When considering the first transformer block and working with learned embeddings and positional encoding, $z'_a(X)$ would be the embedded inputs in the model’s internal representation space. We comment that fixed embedding can be analyzed similarly but requires defining three separate $z'(X)$ -like fields for values, keys, and queries. Kernel evaluation corresponds to propagating the token-to-token covariance matrix, in the sense of Cho & Saul (2009), through the transformer block, starting from the attention layer.

Consider a multi-head attention layer with H heads and inputs $z'_a(X) \in \mathbb{R}^{d_{\text{model}}}$ which we package into $Z'(X) \in \mathbb{R}^{T \times d_{\text{model}}}$. The attention layer’s output at token $a \in [T]$ on input X is

$$z_a(X) = \frac{1}{\sqrt{H}} \sum_{h=1}^H \sum_{c=1}^T A_{ac}^h(X) W_V^h z'_c(X), \quad (3)$$

where

$$A_{ac}^h(X) = \text{Softmax} \left(\frac{1}{\sqrt{d_k}} z'_a(X)^\top W_Q^h (W_K^h)^\top Z'(X)^\top \right)_c \quad (4)$$

are the attention weights. The covariance update requires computing the expectation in Eq. (2) for all pairs $a, b \in [T]$. This involves several Gaussian averages over: z' , query / key weights $W_K^h, W_Q^h \in \mathbb{R}^{d_{\text{model}} \times d_k}$, and value weights $W_V^h \in \mathbb{R}^{d_{\text{model}} \times d_{\text{model}}}$. The latter is straightforward, yielding

$$\mathbb{E}[z_a(X_1)^\top z_b(X_2) | z'] = \frac{1}{H d_{\text{model}}} \sum_{h,j=1}^{H, d_{\text{model}}} \mathbb{E}_{W_Q^h, W_K^h} \left[\sum_{c,e=1}^T \frac{e^{S_{ac}^h(X_1)} [z'_c(X_1)]_j}{\sum_{d=1}^T e^{S_{ad}^h(X_1)}} \frac{e^{S_{be}^h(X_2)} [z'_e(X_2)]_j}{\sum_{f=1}^T e^{S_{bf}^h(X_2)}} \right]. \quad (5)$$

The attention scores are given by

$$S_{ac}^h(X) = \frac{1}{\sqrt{d_k}} \mathbf{z}'_a(X)^\top W_Q^h (W_K^h)^\top \mathbf{z}'_c(X).$$

In the limit $d_{\text{model}}, d_k \rightarrow \infty$, the scores are multivariate zero-centered Gaussians w.r.t. to the ensemble of W_K, W_Q with correlation given by

$$\mathbb{E}_{W_Q^h, W_K^h} [S_{ac}^h(X_1) S_{be}^h(X_2) | \mathbf{z}'] = \left(\frac{\mathbf{z}'_a(X_1)^\top \mathbf{z}'_b(X_2)}{d_{\text{model}}} \right) \left(\frac{\mathbf{z}'_c(X_1)^\top \mathbf{z}'_e(X_2)}{d_{\text{model}}} \right) \quad (6)$$

In the limit, the overlap concentrates to the average, being the following kernel

$$\lim_{d_{\text{model}} \rightarrow \infty} \mathbb{E} \left[\mathbb{E}_{W_Q^h, W_K^h} [S_{ac}^h(X_1) S_{be}^h(X_2) | \mathbf{z}'] \right] = \Sigma'_{ab}(X_1, X_2) \Sigma'_{ce}(X_1, X_2). \quad (7)$$

4.4. Complexity and Accuracy of Kernel Evaluation

Consider the computational complexity of evaluating Eq. (5) using Monte Carlo. One efficient approach proceeds as follows. First, we draw $2T^2$ score samples, according to their multivariate Gaussian distribution. Utilizing the tensor product structure in Eq. (7), this can be done at $O(T^3)$ computational cost instead of the native $O(T^6)$ (see App. D). Producing the attention matrices $A(X_1), A(X_2)$ then requires additional $O(T^2)$ steps. Finally, replacing $d_{\text{model}}^{-1} \sum_{j=1}^{d_{\text{model}}} \mathbf{z}'_c(X_1)_j \mathbf{z}'_e(X_2)_j$ by $\Sigma'_{ce}(X_1, X_2)$, Eq. (5) can be written in matrix form $A(X_1) \Sigma'(X_1, X_2) A(X_2)^\top$, indicating additional $O(T^3)$ operations. The cost of one MC evaluation is thus $O(T^3)$, dominated by matrix multiplication and efficient Cholesky decomposition. Assuming, for simplicity, that this attention layer is the final transformer block, the overall cost of estimating the NNGP kernel predictor becomes $O(PN_{\text{MC}}T^3)$ with MC-induced noise that scales as $O(\sqrt{P/N_{\text{MC}}})$ for a given P .

Considering Eq. (1), we note that α is a property of the training set, agnostic of T at inference. Hence, its magnitude does not scale with T (unless P does). Furthermore, the doubled attention factor being averaged over is bounded in a T -independent manner due to the layer-norm modules ($\max_{c,e} \{\mathbf{z}'_c(X_1)^\top \mathbf{z}'_e(X_2)\} < \infty$). And since the MC-induced noise on the kernel predictor scales as $O(\sqrt{P/N_{\text{MC}}})$, it can be reduced to the desired Δ -accuracy of the outputs, independent of T . As further layers of the transformer block (e.g., MLP) do not mix sequence indices, propagating Σ through those only requires its diagonal elements and has lower complexity (see App. A.3).

In App. E we argue that this scaling of error and compute extend to the full transformer. The crucial observation is

that, while MC error can accumulate across different layers by yielding noisy versions of the true layer-wise Σ' , this accumulation effect is T independent, since the kernel recursion relations of the attention layer and MLP layer have a T -independent Lipschitz constant. Thus, to maintain constant accuracy, one only needs to scale the number of MC samples with depth (L), not with context length (T).

Assume now that a transformer in the infinite width / attention limit has captured an algorithm A under $\mu_{X,T}$. Then, for sufficiently small $\delta > 0$, there exist $T_0 = T_0(\delta)$, $C = C(\delta)$, and $P = P_0(\delta) + C \log(T/T_0)$ such that the kernel predictor f_δ from Eq. (1) satisfies

$$\Pr_{X \sim \mu_{X,T}} [|f_\delta(X) - A(X)| < \Delta/3] \geq 1 - \delta/2$$

for any $T \geq T_0$. Using MC to evaluate $f_\delta(X)$, we get $f_\delta^{\text{MC}}(X)$. Given the MC-induced noise scale, then by the sub-Gaussian tail bound, we have

$$\Pr_{X \sim \mu_{X,T}} [|f_\delta^{\text{MC}}(X) - f_\delta(X)| < \Delta/6] \geq 1 - 2e^{-c\Delta^2 N_{\text{MC}}/P}$$

Applying the triangle inequality, we have

$$\Pr_{X \sim \mu_{X,T}} [|f_\delta^{\text{MC}}(X) - A(X)| < \Delta/2] \geq 1 - 2e^{-c\Delta^2 N_{\text{MC}}/P} - \delta/2,$$

and we want $2e^{-c\Delta^2 N_{\text{MC}}/P} \approx \delta/2$, which imposes $N_{\text{MC}} \propto P \log(1/\delta)$. Evaluating $f_\delta^{\text{MC}}(X)$, as we have argued, requires $O(PN_{\text{MC}}T^3)$. Thus, the infinite width / attention transformer is an EPTHS for the task defined by the algorithm it captured with complexity $O(T^{3+\epsilon})$ for any $\epsilon > 0$ (coming from $\log(T)^2$ w.r.t. $\mu_{X,T}$). Its δ -implementation is given by $f_\delta^{\text{MC}}(X)$, computed in time $O(P^2 \log(1/\delta)T^3)$. Notably, $\Delta/2$ provides a conclusive decision rule.

5. Tighter Bounds and Feature Learning

The above results invite several extensions both in terms of tightness and richness, which we explore here. Unlike in FCNs, kernel evaluation for transformers is far more costly than a forward-pass because it requires tracking correlations over the entire context. In contrast, various bounds on NTK convergence (Huang & Yau, 2020; Jacot et al., 2018; Huang et al., 2021) suggest that, at least for MLPs and CNNs, the discrepancy between the NTK kernel predictor and the finite network scales as P^γ/N for some architecture-dependent constant exponent γ , where N is the architecture “width” or redundancy scale (e.g., width for MLPs, channels for convolutional neural networks, or heads and internal dimensions for transformers).

Notably, however, how well this scaling holds in extreme OOD cases such as ours is, to the best of our knowledge, not

well explored. In the section below, we provide analytical evidence that it nevertheless holds. Given this, if a transformer captured an algorithm, then $P = O(\log(T))$ and N need only scale poly-logarithmically with T . As a result, we can approximate the infinite-width lazy NTK predictor using a forward-pass on a finite trained network with $N \propto \log(T)^\gamma$, getting computational complexity scaling of $O(T^2 \log(T)^\gamma)$ (see App. A.2). This is a tighter upper bound compared to $PN_{\text{MC}}T^3$ discussed in Sec. 4.4. We comment that it can be further improved to $O(T)$ with rank-limited attention.

Turning to the rich learning regime, various works on Bayesian learning view rich learning as lazy learning with adapted pre-activation kernels (Rubin et al., 2025; Bordelon & Pehlevan, 2022; Aitchison, 2021; Sompolinsky, 1988) or weights covariance matrices (Rubin et al., 2025; Ménard et al., 2024). Notably, repeating our previous kernel computation with Gaussian weights having richer covariance bounded by some T -independent constant does not make kernel assessment more complex, thus maintaining $O(T^3 \log(T)^2)$ complexity. We further note that the emergence of learned circuits, whose number may depend polynomially in P , again brings us to T -dependence scaling, as in the forward-pass computation on a finite network.

Finally, we can combine these two extensions by approximating the rich infinite-width NTK predictor using a finite neural network under the assumption that the discrepancy scales as P^γ/N (potentially with $\gamma \approx 0$ (Bordelon & Pehlevan, 2023; Seroussi et al., 2023)). If that is the case, complexity is again upper-bounded by that of the forward-pass.

5.1. Perturbation Theory Estimate

Here, we provide analytic support to the claim that, at least in standard scaling, convergence to the infinite NTK transformer requires $N = \text{poly}(P)$ irrespective of T . This complements existing results (Huang & Yau, 2020; Huang et al., 2021), which assume a fixed input dimension. The crux of the argument detailed below is that, due to the averaging nature of attention, pre-activations, outputs, and gradients do not scale extensively with T .

We proceed by adopting a Bayesian viewpoint and, for simplicity, focus only on predicting the T -th token. We let K denote the T -th output kernel matrix,

$$K_{\mu\nu} = K(X_\mu, X_\nu) \equiv \Sigma_{TT}^{\text{out}}(X_\mu, X_\nu)$$

and $\kappa > 0$ be the ridge parameter / observation noise. The leading order correction, $f_U(X)$, to the posterior predictor on the T -th sequence index,

$$f(X_*) = f_K(X_*) + \frac{1}{N} f_U(X_*) + O(N^{-2}),$$

was given in (Naveh et al., 2021, Eq. (11)) by

$$f_U(X_*) = \frac{1}{6} \tilde{U}_{\mu_1\mu_2\mu_3}^* \left(\tilde{y}_{\mu_1} \tilde{y}_{\mu_2} \tilde{y}_{\mu_3} - 3\tilde{K}_{\mu_1\mu_2}^{-1} \tilde{y}_{\mu_3} \right), \quad (8)$$

where $\tilde{K} = (K + \kappa I_P)$, U is the 4th-order functional cumulant (Naveh et al., 2021) of the output, we let

$$\begin{aligned} \tilde{y}_\mu &:= \tilde{K}_{\mu\nu}^{-1} y_\nu, \\ \tilde{U}_{\mu_1\mu_2\mu_3}^* &:= U_{\mu_1\mu_2\mu_3}^* - U_{\mu_1\mu_2\mu_3\mu_4} \tilde{K}_{\mu_4\nu}^{-1} K_\nu^*, \end{aligned} \quad (9)$$

and all repeating indices are summed over the training set (i.e., $\mu = 1, \dots, P$). An asterisk on the RHS of Eq. (9) denotes evaluation at a test point X_* , namely, $K_\nu^* = K(X_*, X_\nu)$ and $U_{\mu_1\mu_2\mu_3}^* = U(X_*, X_{\mu_1}, X_{\mu_2}, X_{\mu_3})$.

To evaluate the computational complexity of $f_U(X_*)$, we argue that all its tensors and vectors can be bounded by a constant in T . By definition, $y_\mu = O(1)$ and $\tilde{K}_{\mu\nu}^{-1} \leq 1/\kappa$ (see App. B). Consequently, $\tilde{y}_\mu = O(1)$. Next, $K_{\mu\nu}, K_\mu^*$ are bounded as they correspond to the variance of the outputs, which have $O(1)$ bounded Gaussian tails at initialization, irrespective of T . Similarly, due to this Gaussian boundedness, the 4th-order cumulant between any four points, including the test point, also obeys $U_{\mu_1\dots\mu_4} \propto U_{\mu_1\dots\mu_3}^* \propto O(1)$. We further note that $K\tilde{K}^{-1}$ is the Gaussian Process Regression (GPR) inference operator on the training set, namely, $\mathbf{f} = K\tilde{K}^{-1}\mathbf{y}$ for $\mathbf{y} = (y_\mu)$ and $\mathbf{f} = (f(X_\mu))$ in \mathbb{R}^P .

A crude approximation, which is nevertheless sufficient for our purpose, is to replace all summands by $O(1)$, leading to P^3 coming from summations over $\mu_1, \mu_2, \mu_3 \in [P]$ scaling times P^2 from $\mu_4, \nu \in [P]$, totaling $N \propto P^5$. A tighter bound comes from noting that the latter two summations have a simple interpretation: for fixed μ_1, μ_2, μ_3 , $\tilde{U}_{\mu_1, \mu_2, \mu_3}^*$ is the average discrepancy when using GPR to predict $U(\cdot, X_{\mu_1}, X_{\mu_2}, X_{\mu_3})$. One may then use GPR error estimate bounds to turn this extra P^2 dependence into a \sqrt{P} dependence as follows. First, note that, in general, for a function g in the RKHS, $g(X) = \langle g, K(X, \cdot) \rangle_{\mathcal{H}_K}$ and, consequently, $|g(X)| \leq \|g\|_{\mathcal{H}_K} \|K(X, \cdot)\|_{\mathcal{H}_K} = \|g\|_{\mathcal{H}_K} K(X, X)$. Next, replacing $g(X)$ by a GPR predictor, $f_K(X)$, and viewing X as a test point, we may use $f_K(X) = K(X, \cdot)^\top (K + \kappa I_P)^{-1} \mathbf{y}$ and bound $|f_K(X)|$ by its RKHS norm. For the latter, we observe that

$$\|f_K(X)\|_{\mathcal{H}_K}^2 = \mathbf{y}^\top (K + \kappa I_P)^{-1} K (K + \kappa I_P)^{-1} \mathbf{y}. \quad (10)$$

The spectral norm of the middle operator is bounded by $(4\kappa)^{-1}$ (see App. B), and we finally obtain

$$|f_K(X_*)| < \frac{\|\mathbf{y}\|_2}{4\kappa} \cdot K(X_*, X_*) = O(\sqrt{P}), \quad (11)$$

where we assumed properly normalized kernels and target functions. This implies a worst-case $O(\sqrt{P})$ bound on the discrepancy as stated.

6. Experiments

Induction heads. Here we consider a vocabulary of size $V = 1024$ and sequences of length T . For each sequence, we first generate random tokens and select an arbitrary ‘trigger’ token from the vocabulary. To prevent ambiguity, we strictly enforce that the trigger appears only where intended by replacing any pre-existing random occurrences with the subsequent token in the vocabulary (modulo V). We then inject the trigger token at a random index $i_K \in \{0, \dots, T/2 - 1\}$ and again at the final sequence index $T - 1$. The tokens are mapped to learned embeddings ($X \in \mathbb{R}^{T \times d}$) and augmented with Rotary Positional Embeddings (RoPE). The objective is to predict the token following the final trigger. To solve this, the transformer must perform an induction head operation (Elhage et al., 2021): it must locate the previous occurrence of the trigger token (at index i_K) and copy the token immediately following it (x_{i_K+1}).

Algorithmic Sorting. Here we consider a vocabulary of integers $\mathcal{V} = \{0, \dots, 999\}$ and a sequence length T . For each instance, we generate a sequence u of T distinct integers sampled uniformly without replacement from \mathcal{V} . We then construct the full sequence by concatenating the unsorted list u , a special separator token (SEP), and the sorted version of the list s . The inputs are mapped to learned embeddings and augmented with RoPE positional encodings. The model is trained using a standard causal next-token prediction objective over the concatenated sequence $[u, \text{SEP}, s]$. However, we apply a mask to the loss function to ignore predictions on the unsorted prefix u , calculating the loss only on the generation of the separator and the sorted suffix s . Furthermore, accuracy is averaged over tokens. This task forces the model to implement a sorting algorithm: at each step of the generation phase, it must attend back to the unsorted prefix u to identify and copy the next smallest element that has not been generated yet.

Random Geometric Graphs. We test algorithmic capture on two types of combinatorial graph problems. To that end, we generate random (undirected) graph instances following the Random Geometric Graph (RGG) setup (Penrose, 2003). First, we draw $T+2$ points $x_a, a = 0, \dots, T+1$, i.i.d. from a uniform measure μ_x on $[-1, 1]^d$. We consider each x_a as a node in our sampled RGG. The nodes x_0 and x_{T+1} take the special role of source and target, respectively. Next, we fix $r \geq 0$ and add an edge of weight (or capacity) 1 between any two nodes x_a and x_b with $\|x_a - x_b\|_2 \leq r$. Unless stated otherwise, we parametrize r via the expected degree α using Dall & Christensen (2002, Eq. (7)) and choose α near the regime where a giant linear-sized component emerges. We denote our joint input measure by $\mu_{X,T} := \mu_x^{\otimes(T+2)}$. From an average-time or heuristic complexity perspective (Levin, 1986; Impagliazzo, 1995), this distribution has low sampling complexity but generates relatively hard graph

instances.

Geometric Planning (SPP). Consider a finite undirected graph $\mathcal{G} = (\mathcal{V}, \mathcal{E})$ with node set \mathcal{V} of size $V = |\mathcal{V}|$, edge set \mathcal{E} of size $E = |\mathcal{E}|$, and two distinguished nodes: a source v_s and target v_t . A (node) path in \mathcal{G} from source to target is a sequence $\pi = (v_0, \dots, v_n)$ of nodes such that $\{v_{i-1}, v_i\} \in \mathcal{E}$ for $i \in [n]$ beginning with $v_0 = v_s$ and ending with $v_n = v_t$. Graph weighting constitutes a map $c : \mathcal{E} \rightarrow \mathbb{R}_{\geq 0}$. In our RGG setting, weighting is constant $c : \mathcal{E} \rightarrow \{1\}$. The SPP consists of finding an optimal path π^* for

$$\pi^* \in \operatorname{argmin}_{\substack{\pi=(v_0, \dots, v_n) \\ v_0=v_s, v_n=v_t}} \sum_{i=1}^n c(\{v_{i-1}, v_i\}) \quad (12)$$

For our $\mu_{X,T}$, considered at the critical connectivity threshold, average-case time-complexity for source-target SPP is $\mathbb{E}_{X \sim \mu_{X,T}} [t(X)] = \mathbb{E}_{X \sim \mu_{X,T}} [E(X) + V(X)] = O(T \log(T))$, matching standard worst-case complexity for the single-pair SPP on an undirected unit-weight graph using Breadth-First Search (BFS) and critical connectivity expectation $\mathbb{E}_{X \sim \mu_{X,T}} [E(X)] = \Theta(T \log T)$. As noted in Sec. 3, this places the distributional SPP task in the EPTHS class of complexity $O(T^{1+\epsilon})$ under $\mu_{X,T}$ for every $\epsilon > 0$.

MinCut (MaxFlow). Starting from the RGG and graph setup above, we adapt it to add directions to edges, i.e., consider $\mathcal{E} \subseteq \mathcal{V} \times \mathcal{V}$. In a MinCut / MaxFlow network (Bertsekas, 1998, Proposition 3.2), nodes, apart from the source and target, are termed relay nodes. In our directed graph adaptation, relay nodes become bi-directional (with equal capacity), all edges incident to the source have v_s as their initial node, and all edges incident to the target have v_t as their terminal node as in Ramamoorthy et al. (2005, Definition 2).⁵ A cut $\mathcal{S} \subset \mathcal{V}$ in the graph is a subset containing the source $v_s \in \mathcal{S}$ whose complement $\bar{\mathcal{S}} = \mathcal{V} \setminus \mathcal{S}$ contains the target $v_t \in \bar{\mathcal{S}}$. The MinCut problem consists of finding an optimal cut \mathcal{S}^* for

$$\mathcal{S}^* \in \operatorname{argmin}_{\substack{\mathcal{S} \subset \mathcal{V} \\ v_s \in \mathcal{S} \\ v_t \in \bar{\mathcal{S}}}} \sum_{\substack{(v, \bar{v}) \in \mathcal{E} \\ v \in \mathcal{S}, \bar{v} \in \bar{\mathcal{S}}}} c(v, \bar{v}). \quad (13)$$

Average-case for MinCut/MaxFlow is $O(\mathbb{E}[VE])$, matching standard worst-case complexity for MaxFlow (Orlin, 2013). For similar considerations as in SPP, this places MinCut/MaxFlow in the EPTHS class of complexity $O(T^{2+\epsilon})$ under $\mu_{X,T}$ for every $\epsilon > 0$.

⁵Equivalently, we may take the complete directed edge set $\mathcal{E} = \mathcal{V} \times \mathcal{V}$ (optionally excluding self-loops) and extend edge capacity c by setting $c(u, v) = 0$ for all directed pairs $(u, v) \in \mathcal{E}$ not present in the geometric graph; this leaves the MinCut/MaxFlow value unchanged.

7. Discussion

In this work, we moved beyond the question of what transformers can express—which, in the infinite-width limit, is effectively everything—and instead asked what algorithms they can learn to execute. By formally defining Algorithmic Capture as the ability to generalize to arbitrary input sizes (T) with minimal sample adaptation, we offered a distinction between genuine algorithmic learning and statistical interpolation. Our theoretical analysis of infinite-width transformers in both the lazy and rich regimes established a rigorous upper bound on their inference-time computational complexity, effectively limiting them to the class of Efficient Polynomial Time Heuristic Schemes (EPTS), specifically those with complexity scaling no worse than $O(T^{3+\epsilon})$ for $\epsilon > 0$ and most likely $O(T^{2+\epsilon})$.

Our empirical findings illustrate a spectrum of algorithmic capabilities that our framework helps decompose. On the one hand, we observe clear instances of algorithmic capture in tasks like induction heads and sorting, where the algorithmic complexity is low and aligns well with finite circuit solutions and RASP programs. On the other, we find tasks like MinCut, where the algorithmic complexity $O(VE) = O(T^3)$ pushes against our bounds. Other tasks seem allowed by our tighter bounds, but nonetheless were not captured, even at large depth.

This discrepancy highlights a fruitful avenue for future research: refining the estimate of inference-time complexity. Our first bound relies on a “brute force” propagation of kernel covariances, akin to the recursions of Cho & Saul (2009). While robust, this approach may be overly conservative, leaving room for more clever approximations of the kernel. In fact, we conjecture that the dominant spectral weight of the kernel lies in the space of rather simple permutation-invariant sparse functions.⁶

Finally, it would be interesting to generalize these results to deeper or recurring architectures. Just like in the current work, the fact that these deeper nets can express complex algorithms does not mean that they would learn them, as various works and our own experiments with deep transformers suggest. At least for lazy learning, where our bound is largely determined by the complexity of kernel evaluation, this amounts to understanding fixed points of the kernel recursion equations, which are simple for MLPs (Schoenholz et al., 2017) but less well explored for transformers. Such results can serve as a stepping stone to analyze whether faithful algorithmic circuits can evolve under standard supervised learning or reinforcement learning techniques.

⁶To be published.

References

- Abbe, E., Bengio, S., Lotfi, A., and Rizk, K. Generalization on the unseen, logic reasoning and degree curriculum. *Journal of Machine Learning Research*, 25(331):1–58, 2024.
- Aitchison, L. A statistical theory of cold posteriors in deep neural networks. In *International Conference on Learning Representations (ICLR)*, 2021. URL <https://openreview.net/forum?id=Rd138pWXMvG>.
- Anil, C., Wu, Y., Andreassen, A., Lewkowycz, A., Misra, V., Ramasesh, V., Slone, A., Gur-Ari, G., Dyer, E., and Neyshabur, B. Exploring length generalization in large language models. In *Advances in Neural Information Processing Systems (NeurIPS)*, volume 35, pp. 38546–38556, 2022. URL https://proceedings.neurips.cc/paper_files/paper/2022/hash/f96180a6b7d142d76f827a5d7367c3b2-Abstract-Conference.html.
- Barak, B., Edelman, B. L., Goel, S., Kakade, S., Malach, E., and Zhang, C. Hidden progress in deep learning: Sgd learns parities near the computational limit. In *Advances in Neural Information Processing Systems*, volume 35, 2022. URL https://proceedings.neurips.cc/paper_files/paper/2022/file/884baf65392170763b27c914087bde01-Paper-Conference.pdf.
- Bennani, M. A., Doan, T., and Sugiyama, M. Generalization guarantees for continual learning with orthogonal gradient descent. *arXiv preprint arXiv:2006.11942*, 2020.
- Bertsekas, D. P. *Network Optimization: Continuous and Discrete Models*. Athena Scientific, Belmont, MA, 1998. ISBN 1-886529-02-7. URL <http://www.athenasc.com/netopt.html>.
- Bietti, A., Bruna, J., Sanford, C., and Song, M. J. Learning single-index models with shallow neural networks. *Advances in Neural Information Processing Systems*, 35:9768–9780, 2022. URL https://proceedings.neurips.cc/paper_files/paper/2022/file/3fb6c52aeb11e09053c16eabee74dd7b-Paper-Conference.pdf.
- Bogdanov, A. and Trevisan, L. Average-case complexity. *Foundations and Trends in Theoretical Computer Science*, 2(1):1–106, 2006. doi: 10.1561/0400000004.
- Bordelon, B. and Pehlevan, C. Self-consistent dynamical field theory of kernel evolution in wide neural networks. In *Advances in Neural Information Processing Systems (NeurIPS)*, volume 35, pp. 32240–32256,

2022. URL https://proceedings.neurips.cc/paper_files/paper/2022/hash/d14b434b92b0286372bf906e5300d60d-Abstract.html.
- Bordelon, B. and Pehlevan, C. Dynamics of finite width kernel and prediction fluctuations in mean field neural networks, 2023. URL <https://arxiv.org/abs/2304.03408>.
- Chen, L., Peng, B., and Wu, H. Theoretical limitations of multi-layer transformer. *arXiv preprint arXiv:2412.02975*, 2024. URL <https://arxiv.org/abs/2412.02975>.
- Chiang, D., Cholak, P., and Pillay, A. Tighter bounds on the expressivity of transformer encoders. In *Proceedings of the 40th International Conference on Machine Learning (ICML)*, volume 202, pp. 5544–5562. PMLR, 2023. URL <https://proceedings.mlr.press/v202/chiang23a.html>.
- Cho, Y. and Saul, L. Kernel methods for deep learning. In *Advances in Neural Information Processing Systems (NIPS)*, volume 22, pp. 342–350, 2009. URL <https://proceedings.neurips.cc/paper/2009/hash/5751ec3e9a4feab575962e78e006250d-Abstract.html>.
- Dall, J. and Christensen, M. Random geometric graphs. *Physical Review E*, 66(1):016121, 2002. doi: 10.1103/PhysRevE.66.016121.
- Dingle, K., Camargo, C. Q., and Louis, A. A. Input–output maps are strongly biased towards simple outputs. *Nature Communications*, 9(1):761, 2018. doi: 10.1038/s41467-018-03101-6. URL <https://doi.org/10.1038/s41467-018-03101-6>.
- Dong, Y., Cordonnier, J.-B., and Loukas, A. Attention is not all you need: Pure attention loses rank doubly exponentially with depth. In *Proceedings of the 38th International Conference on Machine Learning (ICML)*, volume 139, pp. 2793–2803. PMLR, 2021. URL <https://proceedings.mlr.press/v139/dong21a.html>.
- Elhage, N., Nanda, N., Olsson, C., Henighan, T., Joseph, N., Mann, B., Askell, A., Bai, Y., Chen, A., Conerly, T., DasSarma, N., Drain, D., Ganguli, D., Hatfield-Dodds, Z., Hernandez, D., Jones, A., Kernion, J., Lovitt, L., Ndousse, K., Amodei, D., Brown, T., Clark, J., Kaplan, J., McCandlish, S., and Olah, C. A mathematical framework for transformer circuits. *Transformer Circuits Thread*, 2021. URL <https://transformer-circuits.pub/2021/framework/index.html>.
- Ghorbani, B., Mei, S., Misiakiewicz, T., and Montanari, A. When do neural networks outperform kernel methods? *Advances in Neural Information Processing Systems*, 33: 14820–14830, 2020. URL <https://proceedings.neurips.cc/paper/2020/file/a9df2255ad642b923d95503b9a7958d8-Paper.pdf>.
- Gromov, A., Tirumala, K., Shapourian, H., Glorioso, P., and Roberts, D. A. The unreasonable ineffectiveness of the deeper layers. In *International Conference on Learning Representations (ICLR)*, 2025. URL <https://openreview.net/forum?id=XJ2ZqJ2s4d>. Also available as arXiv:2403.17887.
- Hron, J., Bahri, Y., Sohl-Dickstein, J., and Novak, R. Infinite attention: NNGP and NTK for deep attention networks. In *Proceedings of the 37th International Conference on Machine Learning (ICML)*, volume 119, pp. 4376–4386. PMLR, 2020. URL <https://proceedings.mlr.press/v119/hron20a.html>.
- Huang, J. and Yau, H.-T. Dynamics of deep neural networks and neural tangent hierarchy. In *International conference on machine learning*, pp. 4542–4551. PMLR, 2020.
- Huang, W., Du, W., and Xu, R. Y. D. On the neural tangent kernel of deep networks with orthogonal initialization, 2021. URL <https://arxiv.org/abs/2004.05867>.
- Impagliazzo, R. A personal view of average-case complexity. In *Proceedings of the 10th Annual Structure in Complexity Theory Conference*, pp. 134–147. IEEE, 1995. doi: 10.1109/SCT.1995.514853.
- Jacot, A., Gabriel, F., and Hongler, C. Neural tangent kernel: Convergence and generalization in neural networks. In *Advances in Neural Information Processing Systems (NeurIPS)*, volume 31, pp. 8571–8580, 2018. URL <https://proceedings.neurips.cc/paper/2018/hash/5a4be1fa34e62bb8a6ec6b91d2462f5a-Abstract.html>.
- Lee, J., Bahri, Y., Novak, R., Schoenholz, S., Pennington, J., and Sohl-Dickstein, J. Deep neural networks as gaussian processes. In *International Conference on Learning Representations (ICLR)*, 2018. URL <https://openreview.net/forum?id=B1EA-M-0Z>.
- Levin, L. A. Average case complete problems. *SIAM Journal on Computing*, 15(1):285–286, 1986. doi: 10.1137/0215020.
- Ménard, B., Mallat, S., and Chizat, L. A rainbow in deep network black boxes. *Journal of Machine Learning*

- Research*, 25(141):1–59, 2024. URL <http://jmlr.org/papers/v25/23-1573.html>.
- Merrill, W., Sabharwal, A., and Smith, N. A. Saturated transformers are constant-depth threshold circuits. *Transactions of the Association for Computational Linguistics*, 10:843–856, 2022. doi: 10.1162/tacl.a.00492.
- Mirzadeh, I., Alizadeh, K., Shahrokhi, H., Tuzel, O., Bengio, S., and Farajtabar, M. GSM-symbolic: Understanding the limitations of mathematical reasoning in large language models. In *International Conference on Learning Representations (ICLR)*, 2025. URL <https://openreview.net/forum?id=u21fk4h5YQ>. Also available as arXiv:2410.05229.
- Nanda, N., Chan, L., Lieberum, T., Smith, J., and Steinhart, J. Progress measures for grokking via mechanistic interpretability. In *International Conference on Learning Representations*, 2023. URL <https://openreview.net/pdf?id=9XFSbDPmdW>.
- Naveh, G., Ben David, O., Sompolinsky, H., and Ringel, Z. Predicting the outputs of finite deep neural networks trained with noisy gradients. *Phys. Rev. E*, 104:064301, Dec 2021. doi: 10.1103/PhysRevE.104.064301. URL <https://link.aps.org/doi/10.1103/PhysRevE.104.064301>.
- Orlin, J. B. Max flows in $O(nm)$ time, or better. In *Proceedings of the 45th Annual ACM Symposium on Theory of Computing (STOC)*, pp. 765–774, 2013. doi: 10.1145/2488608.2488705.
- Penrose, M. *Random Geometric Graphs*, volume 5 of *Oxford Studies in Probability*. Oxford University Press, 2003. ISBN 9780198506263.
- Power, A., Burda, Y., Edwards, H., Babuschkin, I., and Misra, V. Grokking: Generalization beyond overfitting on small algorithmic datasets. *arXiv preprint arXiv:2201.02177*, 2022. URL <https://arxiv.org/abs/2201.02177>.
- Ramamoorthy, A., Shi, J., and Wesel, R. D. On the capacity of network coding for random networks. *IEEE Transactions on Information Theory*, 51(8):2878–2885, 2005. doi: 10.1109/TIT.2005.851722.
- Rubin, N., Davidovich, O., and Ringel, Z. Mitigating the curse of detail: Scaling arguments for feature learning and sample complexity. *arXiv preprint arXiv:2512.04165*, 2025. URL <https://arxiv.org/abs/2512.04165>.
- Schoenholz, S. S., Gilmer, J., Ganguli, S., and Sohl-Dickstein, J. Deep information propagation. In *International Conference on Learning Representations (ICLR)*, 2017. URL <https://openreview.net/forum?id=H1W1UN9gg>.
- Seroussi, I., Naveh, G., and Ringel, Z. Separation of scales and a thermodynamic description of feature learning in some cnns. *Nature Communications*, 14(1):908, 2023. doi: 10.1038/s41467-023-36361-y. URL <https://doi.org/10.1038/s41467-023-36361-y>.
- Sompolinsky, H. Statistical mechanics of neural networks. *Physics Today*, 41(12):40–52, 1988. doi: 10.1063/1.881142.
- Valle-Pérez, G., Camargo, C. Q., and Louis, A. A. Deep learning generalizes because the parameter-function map is biased towards simple functions, 2019. URL <https://arxiv.org/abs/1805.08522>.
- Veličković, P., Ying, R., Padovano, M., Hadsell, R., and Blundell, C. Neural execution of graph algorithms. In *International Conference on Learning Representations*, 2020. URL <https://openreview.net/forum?id=SkqK00Etvs>.
- von Mises, R. *Mathematical Theory of Probability and Statistics*. Academic Press, New York and London, 1964.
- Wei, C., Lee, J. D., Liu, Q., and Ma, T. Regularization matters: Generalization and optimization of neural nets v.s. their induced kernel. In *Advances in Neural Information Processing Systems*, volume 32, 2019. URL <https://arxiv.org/abs/1810.05369>.
- Weiss, G., Goldberg, Y., and Yahav, E. Thinking like transformers, 2021. URL <https://arxiv.org/abs/2106.06981>.
- Xu, K., Li, J., Zhang, M., Du, S. S., Kawarabayashi, K.-i., and Jegelka, S. What can neural networks reason about? *arXiv preprint arXiv:1905.13211*, 2019.
- Xu, K., Zhang, M., Li, J., Du, S. S., Kawarabayashi, K.-i., and Jegelka, S. How neural networks extrapolate: From feedforward to graph neural networks. *arXiv preprint arXiv:2009.11848*, 2020.
- Zhou, H., Bradley, A., Littwin, E., Razin, N., Saremi, O., Susskind, J. M., Bengio, S., and Nakkiran, P. What algorithms can transformers learn? a study in length generalization. In *The Twelfth International Conference on Learning Representations*, 2024. URL <https://openreview.net/forum?id=AssIuHnmHX>.

A. Transformers in Detail

A.1. Setup

As stated, we focus on decoder-only transformers with softmax self-attention and no causal masking. We consider a multi-layer, multi-head transformer with L transformer blocks and H heads each. Each transformer block is defined as follows. For the block input $X \in \mathbb{R}^{T \times d_{\text{model}}}$, we define the pre-activation

$$Z(X) = \frac{1}{\sqrt{H}} \sum_{h=1}^H A^h(X) V^h(X) \in \mathbb{R}^{T \times d_{\text{model}}} \quad (14)$$

with attention weights

$$A^h(X) = \text{Softmax} \left(\frac{1}{\sqrt{d_k}} Q^h(X) K^h(X)^\top \right) \in \mathbb{R}^{T \times T}$$

In particular, for $a \in [T]$,

$$z_a(X) = \frac{1}{\sqrt{H}} \sum_{h=1}^H \sum_{b=1}^T A_{ab}^h(X) V_b^h(X) \in \mathbb{R}^{d_{\text{model}}}$$

where

$$\begin{aligned} Q^h(X) &= X W_Q^h \in \mathbb{R}^{T \times d_k} \\ K^h(X) &= X W_K^h \in \mathbb{R}^{T \times d_k} \\ V^h(X) &= X W_V^h \in \mathbb{R}^{T \times d_{\text{model}}} \end{aligned}$$

for $W_Q^h, W_K^h \in \mathbb{R}^{d_{\text{model}} \times d_k}$ and $W_V^h \in \mathbb{R}^{d_{\text{model}} \times d_{\text{model}}}$, with each weight matrix entry sampled i.i.d. $(W_Q^h)_{i,j}, (W_K^h)_{i,j}, (W_V^h)_{i,j} \sim \mathcal{N}(0, 1/d_{\text{model}})$. Adding an MLP layer (or, more generally, some form of non-linearity), the output of the transformer block at the a -th token is given by

$$\text{MLP}(z_a) = \phi(z_a) W + \mathbf{b}$$

for an activation function ϕ (e.g., ReLU), $W \in \mathbb{R}^{d_{\text{model}} \times d_{\text{model}}}$, and $\mathbf{b} \in \mathbb{R}^{d_{\text{model}}}$. As input to the initial block, we will add an embedding from raw input dimension into the model's internal representation space $W_{\text{emb}} : \mathbb{R}^d \rightarrow \mathbb{R}^{d_{\text{model}}}$.

This setup is intentionally simplified: we omit positional encoding, layer normalization, and the standard two-layer FFN/MLP (using instead a single pointwise nonlinearity followed by a linear map). We also omit the usual output projection W_O , combining heads by averaging as in (14).

A.2. Inference-time Complexity

The inference-time complexity of a transformer is $O(T^2)$ as we will now demonstrate. First, note that the number of FLOPs involved in multiplying matrices $(m, k) \times (k, n)$ is $\approx 2mkn$. Therefore, calculating $Q(X), K(X)$ is \approx

$2Td_{\text{model}}d_k$, and calculating $V(X)$ is $\approx 2Td_{\text{model}}^2$. Thus, calculating $Q(X)K(X)^\top$ is $\approx 2T^2d_k$. Calculating Softmax is $\Theta(T^2)$, while multiplying by $V(X)$ is $\approx 2T^2d_{\text{model}}$. Thus, for the attention layer in a transformer block, we get

$$\begin{aligned} \text{FLOPs}_{\text{attn}} &\approx H(4Td_{\text{model}}d_k + \\ &2Td_{\text{model}}^2 + 2T^2d_k + \Theta(T^2) + 2T^2d_{\text{model}}). \end{aligned}$$

As for the MLP block, $\text{FLOPs}_{\text{MLP}} \approx 2Td_{\text{model}}^2$. And together, we get

$$\begin{aligned} \text{FLOPs}_{\text{block}} &= \\ &O(H [Td_{\text{model}}d_k + Td_{\text{model}}^2 + T^2(d_k + d_{\text{model}})]) \end{aligned}$$

For a typical choice $d_k = d_{\text{model}}/H$, we get

$$\text{FLOPs}_{\text{block}} = O(H [Td_{\text{model}}^2 + T^2d_{\text{model}}])$$

And for a transformer with L blocks

$$\text{FLOPs}_{\text{trans}} = O(LH [Td_{\text{model}}^2 + T^2d_{\text{model}}]).$$

Following our discussion in 5, when $d_{\text{model}} \propto \log(T)^\gamma$ and $H = O(1)$, we have computational complexity scaling of T^2 times negligible logarithmic corrections.

A.3. Kernel Propagation

Kernel propagation through network layers was considered in (Lee et al., 2018) for deep FCNs. Their propagation rule (Lee et al., 2018, Eq. (4)) applies, in our case, as we pass through the MLP layer

$$\begin{aligned} \mathbb{E}[\text{MLP}(z_a(X_1))^\top \text{MLP}(z_b(X_2))] &= \\ \sigma_{\mathbf{b}}^2 + \sigma_W^2 \mathbb{E}_{(z_a(X_1), z_b(X_2)) \sim \mathcal{N}(0, k)} [\phi(z_a(X_1)) \phi(z_b(X_2))] \end{aligned}$$

where $\mathcal{N}(0, k)$ is the bi-variate Gaussian distribution with the 2×2 covariance matrix k define via

$$\begin{aligned} k_{aa} &= \Sigma_{aa}(X_1, X_2), \\ k_{ab} &= k_{ba} = \Sigma_{ab}(X_1, X_2), \\ k_{bb} &= \Sigma_{bb}(X_1, X_2). \end{aligned}$$

In this sense, propagating Σ_{ab} through the MLP only requires its diagonal elements and has lower complexity.

B. Kernel Bounds

By Cho & Saul (2009, Theorem 3), in the infinite width / attention limit $z_T^{\text{out}} \sim \mathcal{GP}(0, \Sigma_T^{\text{out}})$, which results in the GPR predictor

$$\begin{aligned} z_T^{\text{out}}(X_*) | \{X_\nu\}_{\nu=1}^P, \mathbf{y} \sim \\ \mathcal{N}(K^* \tilde{K}^{-1} \mathbf{y}, k^* - K^* \tilde{K}^{-1} (K^*)^\top), \end{aligned}$$

conditioned on the dataset, with symmetric PD $\tilde{K} = K + \kappa I_P$ ($\kappa > 0$), the vector of covariances $K^* = (K_{\nu}^*) \equiv (\Sigma_{TT}^{\text{out}}(X_*, X_{\nu})) \in \mathbb{R}^P$, and $k^* = \Sigma_{TT}^{\text{out}}(X_*, X_*) \in \mathbb{R}$.

Now, consider the spectral norm of \tilde{K}^{-1} . It is known that

$$\|\tilde{K}^{-1}\|_2 = \sup \left\{ \left| \mathbf{x}_1^\top \tilde{K}^{-1} \mathbf{x}_2 \right| \mid \mathbf{x}_i \in \mathbb{R}^P : \|\mathbf{x}_1\| = 1 = \|\mathbf{x}_2\| \right\}.$$

Choosing $\mathbf{x}_1 = e_\mu$ and $\mathbf{x}_2 = e_\nu$, we get

$$\left| \tilde{K}_{\mu\nu}^{-1} \right| \leq \left\| \tilde{K}^{-1} \right\|_2.$$

Using the fact that K is symmetric PSD and \tilde{K} is symmetric PD, we have

$$\text{Spec}(\tilde{K}^{-1}) = \left\{ \frac{1}{\lambda + \kappa} \mid \lambda \in \text{Spec}(K) \right\},$$

so that

$$\left| \tilde{K}_{\mu\nu}^{-1} \right| \leq \left\| \tilde{K}^{-1} \right\|_2 = \max \text{Spec}(\tilde{K}^{-1}) \leq \frac{1}{\kappa}.$$

As for the $P \times P$ matrix establishing the RKHS norm in Eq. (10), we can play a similar game with

$$\text{Spec}(\tilde{K}^{-1} K \tilde{K}^{-1}) = \left\{ \frac{\lambda}{(\lambda + \kappa)^2} \mid \lambda \in \text{Spec}(K) \right\}.$$

Thus,

$$\left\| \tilde{K}^{-1} K \tilde{K}^{-1} \right\|_2 = \max \text{Spec}(\tilde{K}^{-1} K \tilde{K}^{-1}) \leq \frac{1}{4\kappa}.$$

C. Further Experimental Details

We trained all models using a standard decoder-only transformer architecture with GeLU activation. We used embedding dimensions of $d = 256$ and 128 , number of layer $L = 2, 4, 40$, and $H = 4$ attention heads in each block. For Sorting and Induction, the models utilized Rotary Positional Embeddings (RoPE) to capture relative position information. Training was performed online using the Adam optimizer with a learning rate of 10^{-3} and a batch size of $B = 512, 1024$.

For each task, we followed a two-phase protocol: (1) pre-training, where the model was trained on a fixed input size T_0 until it reached a specified accuracy threshold (δ), and (2) adaptation, where the pre-trained weights were fine-tuned and evaluated on larger input sizes $T > T_0$. In all of these experiments, the sample size was computed as the number of epochs times the size of the batch. The sample size (P) reported in Fig. 1 contains only the adaptation cost to larger instances.

For induction we used $d = 256, L = 2, B = 512$; for sorting $d = 128, L = 4, B = 512$; for shallow SPP we used $d = 128, L = 4, B = 1024$; for deep SPP we used $d = 128, L = 4, B = 1024$; for shallow MinCut we used $d = 128, L = 4, B = 1024$; for deep MinCut we used $d = 128, L = 40, B = 1024$.

D. Complexity of Score Draws

The attention kernel estimation involves sampling $2T^2$ scores, $S_{ac}(X_1)$ and $S_{be}(X_2)$, which are multivariate Gaussians in the kernel limit. For this purpose, we utilize Kronecker-structured covariance as well as conditioning in multivariate Gaussians to analyze its computational complexity. First, we consider $S(X_1) \in \mathbb{R}^{T \times T}$. Then

$$\text{vec}(S(X_1)) \sim \mathcal{N}(0, \Theta(X_1, X_1))$$

with $\Theta(X_1, X_1) = \Sigma'(X_1, X_1) \otimes \Sigma'(X_1, X_1)$ as in Eq. (7). Note that $\Sigma'(X_1, X_1) \succeq 0$ by definition and consequently $\Theta(X_1, X_1) \succeq 0$. Given a Cholesky decomposition $\Sigma'(X_1, X_1) = L_1 L_1^\top$, we can decompose $\Theta(X_1, X_1) = (L_1 \otimes L_1)(L_1 \otimes L_1)^\top$. An $S(X_1)$ sample can then be generated at a cost of $O(T^3)$ via $S(X_1) = L_1 U L_1^\top$ for $U_{ab} \stackrel{\text{i.i.d.}}{\sim} \mathcal{N}(0, 1)$.

Next, we apply Bayes' rule

$$p(S(X_1), S(X_2)) = p_S(X_1) p_S(X_2) | S(X_1).$$

The joint covariance of $(S(X_1), S(X_2))$ is the block matrix

$$\begin{pmatrix} \Theta_{11} & \Theta_{12} \\ \Theta_{21} & \Theta_{22} \end{pmatrix} = \begin{pmatrix} \Sigma'_{11} \otimes \Sigma'_{11} & \Sigma'_{12} \otimes \Sigma'_{12} \\ \Sigma'_{21} \otimes \Sigma'_{21} & \Sigma'_{22} \otimes \Sigma'_{22} \end{pmatrix} \succeq 0$$

where $\Sigma'_{ij} \equiv \Sigma'(X_i, X_j)$. The conditional distribution of $S(X_2)$ given $S(X_1)$ is known (von Mises, 1964, Sec. 9.3) to be

$$\begin{aligned} S(X_2) | S(X_1) &\sim \mathcal{N}(M_{\text{cond}}, \Theta_{\text{cond}}) \\ M_{\text{cond}} &= \Theta_{21} \Theta_{11}^{-1} \text{vec}(S(X_1)) \\ \Theta_{\text{cond}} &= \Theta_{22} - \Theta_{21} \Theta_{11}^{-1} \Theta_{12} \succeq 0 \end{aligned}$$

which involves calculating

$$M_{\text{cond}} = \Sigma'_{21} (\Sigma'_{11})^{-1} S(X_1) (\Sigma'_{21} (\Sigma'_{11})^{-1})^\top$$

and $\Sigma'_{21} (\Sigma'_{11})^{-1} \Sigma'_{21}$ for Θ_{cond} , again, at a cost of $O(T^3)$.⁷

To draw a sample from the conditioned Gaussian, we will assume $\Sigma'_{11}, \Sigma'_{22} \succ 0$. We can then calculate

$$H := L_2^{-1} \Sigma'_{21} (\Sigma'_{11})^{-1} \Sigma'_{21} (L_2^\top)^{-1}$$

⁷If Σ'_{11} is not positive definite (PD), we can use the Moore-Penrose pseudo-inverse and the conditional becomes degenerate.

for a Cholesky decomposition $\Sigma'_{22} = L_2 L_2^\top$ at a cost of $O(T^3)$. Then we have

$$((L_2^\top)^{-1} \otimes (L_2)^{-1}) \Theta_{\text{cond}} ((L_2)^{-1} \otimes (L_2^\top)^{-1}) = I \otimes I - H \otimes H.$$

Since the LHS is PSD, we have $I - H \succeq 0$. Consequently, if we diagonalize $H = Q \Lambda Q^{-1}$ with $\Lambda = \text{diag}(\boldsymbol{\lambda})$ and $\boldsymbol{\lambda} = (\lambda_1, \dots, \lambda_T)$, then we can generate a sample at a cost of $O(T^3)$ with

$$S(X_2)|S(X_1) = M_{\text{cond}} + L_2 Q \Delta Q^\top L_2^\top \\ \Delta := \sqrt{\mathbf{1}\mathbf{1}^\top - \boldsymbol{\lambda}\boldsymbol{\lambda}^\top} \odot Q^{-1} U (Q^\top)^{-1}$$

for $U_{ab} \stackrel{\text{i.i.d.}}{\sim} \mathcal{N}(0, 1)$, where \odot is matrix element-wise product. To conclude, we obtain a sample of $(S(X_1), S(X_2))$ at an overall cost of $O(T^3)$.

E. Lipschitz Constant of the MLP and Attention Layer Recursions

In Sec. 4.4, we established that a single MC estimation of the [Cho & Saul \(2009\)](#) kernel for the attention layer, using N_{MC} samples, yields an estimation error bounded by $O(1/\sqrt{N_{\text{MC}}})$ irrespective of the sequence length T . However, evaluating the kernel of a deep transformer involves a sequential chain of estimations, where the empirically evaluated covariance matrix from layer ℓ is passed into the non-linear Gaussian expectations of layer $\ell + 1$. A critical theoretical concern is whether the accumulation of MC errors across layers magnifies extensively with the sequence length T . If the error magnification were to scale as $O(T^k)$, maintaining a constant target accuracy at the network's output would require the number of MC samples N_{MC} to grow polynomially or above with T , thereby invalidating our inference complexity bounds. Here we show that this does not occur. We show that the layer-to-layer kernel recursion maps for both the attention and MLP layers are Lipschitz continuous with respect to the matrix max-norm, and, crucially, that their Lipschitz constants are strictly $O(1)$ and independent of T .

We will let Σ' denote the true pre-activation covariance matrix at a given layer, while $\Sigma' + \Delta\Sigma'$ will be its MC estimate, with a max-norm estimation error of $\|\Delta\Sigma'\|_\infty = \max_{a,b} |\Delta\Sigma'_{ab}|$. Because standard transformer architectures employ LayerNorm, the pre-activation covariance elements are strictly bounded by a constant, which we denote by $\|\Sigma'\|_\infty \leq M = O(1)$.

E.1. Error Propagation in the Attention Layer

Let us pick a pair of tokens $a, b \in [T]$ and of inputs $X_1, X_2 \in \mathbb{R}^{T \times d}$ and denote $\mathbf{s}_1 := S_{a^\bullet}^{h=1}(X_1)$ and $\mathbf{s}_2 :=$

$S_{b^\bullet}^{h=1}(X_2)$, both considered random vectors in \mathbb{R}^T .⁸ By Eq. (5), the exact attention kernel recursion is given by

$$\Sigma_{ab}(X_1, X_2) = \mathbb{E}_{(\mathbf{s}_1, \mathbf{s}_2)} [f(\mathbf{s}_1, \mathbf{s}_2)], \\ f(\mathbf{s}_1, \mathbf{s}_2) := \sum_{c,e=1}^T A_c(\mathbf{s}_1) \Sigma'_{ce}(X_1, X_2) A_e(\mathbf{s}_2)$$

where $A(\mathbf{s}_i)_c = \text{Softmax}(\mathbf{s}_i)_c$, and the $2T$ -dimensional random vector $\tilde{\mathbf{s}} := (\mathbf{s}_1, \mathbf{s}_2)$ follows a multivariate Gaussian distribution $\mathcal{N}(0, C)$ with covariance matrix $C \in \mathbb{R}^{2T \times 2T}$.

A perturbation introduced in the previous layer affects the attention layer output in two ways: it shifts $\Sigma' \rightarrow \Sigma' + \Delta\Sigma'$ and $C \rightarrow C + \Delta C$. We can then bound the total discrepancy $\Delta\Sigma_{ab}(X_1, X_2)$ using the triangle inequality

$$|\Delta\Sigma_{ab}(X_1, X_2)| \leq e_{\text{val}} + e_{\text{measure}}. \quad (15)$$

where the first contribution comes from the direct effect on Σ'_{ce} in $f(\mathbf{s}_1, \mathbf{s}_2)$ and the second from the indirect effect via $A_c(\mathbf{s}_1)$

1. Bounding e_{val} . The error induced by substituting $\Sigma' \rightarrow \Sigma' + \Delta\Sigma'$ is

$$e_{\text{val}} = \left| \mathbb{E}_{\tilde{\mathbf{s}} \sim \mathcal{N}(0, C + \Delta C)} \left[\sum_{c,e=1}^T A_c(\mathbf{s}_1) \Delta\Sigma'_{ce} A_e(\mathbf{s}_2) \right] \right| \\ \leq \|\Delta\Sigma'\|_\infty \mathbb{E}_{(\mathbf{s}_1, \mathbf{s}_2)} \left[\left(\sum_{c=1}^T A_c(\mathbf{s}_1) \right) \left(\sum_{e=1}^T A_e(\mathbf{s}_2) \right) \right] \\ \leq \|\Delta\Sigma'\|_\infty, \quad (16)$$

The 2nd inequality results from Softmax outputs summing up to 1. The valuation error, thus, perfectly absorbs the T^2 summands and is exactly 1-Lipschitz and independent of T .

2. Bounding e_{measure} Next, we evaluate the shift in the expectation due to the perturbed distribution of $\tilde{\mathbf{s}}$. As established in Eq. (7), the covariance C factorizes as

$$C_{(i,c),(j,e)} = (\Sigma'_{ij})_{ab} (\Sigma'_{ij})_{ce}.$$

where, $\Sigma'_{ij} \equiv \Sigma'(X_i, X_j)$. Under perturbation, the corresponding score covariance block is shifted

$$C_{(i,c),(j,e)} \rightarrow ((\Sigma'_{ij})_{ab} + (\Delta\Sigma'_{ij})_{ab}) ((\Sigma'_{ij})_{ce} + (\Delta\Sigma'_{ij})_{ce}).$$

The difference in the score covariance matrices is then

$$\Delta C_{(i,c),(j,e)} = (\Sigma'_{ij})_{ab} (\Delta\Sigma'_{ij})_{ce} + (\Delta\Sigma'_{ij})_{ab} (\Sigma'_{ij})_{ce} + (\Delta\Sigma'_{ij})_{ab} (\Delta\Sigma'_{ij})_{ce}.$$

⁸Taking the expectation over $h = 1, \dots, H$ implies that we may choose a single head to evaluate for, here, chosen arbitrarily to be $h = 1$.

Using $\|\Sigma'\|_\infty \leq M$, we have

$$\|\Delta C\|_\infty \leq 2M \|\Delta\Sigma'\|_\infty + \|\Delta\Sigma'\|_\infty^2. \quad (17)$$

To bound the shift in expectation under the perturbed Gaussian measure, we employ a multivariate Gaussian interpolation technique – a standard application of Gaussian integration by parts, often associated with Price’s Theorem. We construct a continuous interpolation between the unperturbed covariance C and the perturbed covariance $C + \Delta C$ parameterized by $t \in [0, 1]$:

$$C(t) := C + t\Delta C. \quad (18)$$

Let $f(\tilde{\mathbf{S}}(t)) = \sum_{c,e=1}^T A_c(\mathbf{S}^{(1)}(t))A_e(\mathbf{S}^{(2)}(t))\Sigma'_{ce}$ and $\tilde{\mathbf{S}}(t) = (\mathbf{S}^{(1)}(t), \mathbf{S}^{(2)}(t)) \sim \mathcal{N}(0, C(t))$ be a Gaussian random vector defined along this path, and let us define the expected value of our function as a parameterized scalar function of t :

$$\varphi(t) = \mathbb{E}_{\tilde{\mathbf{S}}(t)} \left[f(\tilde{\mathbf{S}}) \right]. \quad (19)$$

The total error introduced by the measure pathway is the absolute difference at the endpoints, $\mathcal{E}_{\text{measure}} = |\varphi(1) - \varphi(0)|$. By the fundamental theorem of calculus, this is bounded by the absolute integral of its derivative:

$$\mathcal{E}_{\text{measure}} = \left| \int_0^1 \varphi'(t) dt \right| \leq \int_0^1 |\varphi'(t)| dt. \quad (20)$$

To compute $\varphi'(t)$, we utilize Price’s Theorem, which establishes that for a twice-differentiable function f , the derivative of its Gaussian expectation with respect to the covariance elements is exactly half the expectation of its corresponding second spatial derivatives. Applying the multivariate chain rule yields:

$$\begin{aligned} \varphi'(t) &= \sum_{i,j,c,e=1}^{2,2,T,T} \frac{dC_{(i,c),(j,e)}(t)}{dt} \frac{\partial}{\partial C_{(i,c),(j,e)}} \mathbb{E}_{\tilde{\mathbf{S}}(t)} \left[f(\tilde{\mathbf{S}}) \right] \\ &= \frac{1}{2} \sum_{i,j,c,e=1}^{2,2,T,T} \Delta C_{(i,c),(j,e)} \mathbb{E}_{\tilde{\mathbf{S}}(t)} \left[\frac{\partial^2 f(\tilde{\mathbf{S}})}{\partial \tilde{S}_{(i,c)} \partial \tilde{S}_{(j,e)}} \right], \end{aligned} \quad (21)$$

Substituting this back into the integral, we can apply the triangle inequality to bring the absolute value inside the expectation. We then bound each covariance perturbation by the matrix max-norm, $|\Delta C_{(i,c),(j,e)}| \leq \|\Delta C\|_\infty$, and

pull this constant outside the summation:

$$\begin{aligned} \mathcal{E}_{\text{measure}} &\leq \quad (22) \\ &\frac{1}{2} \int_0^1 \sum_{i,j,c,e} |\Delta C_{(i,c),(j,e)}| \left| \mathbb{E}_{\tilde{\mathbf{S}}(t)} \left[\frac{\partial^2 f(\tilde{\mathbf{S}})}{\partial \tilde{S}_{(i,c)} \partial \tilde{S}_{(j,e)}} \right] \right| dt \\ &\leq \frac{1}{2} \|\Delta C\|_\infty \int_0^1 \mathbb{E}_{\tilde{\mathbf{S}}(t)} \left[\sum_{i,j,c,e} \left| \frac{\partial^2 f(\tilde{\mathbf{S}})}{\partial \tilde{S}_{(i,c)} \partial \tilde{S}_{(j,e)}} \right| \right] dt. \end{aligned} \quad (23)$$

Finally, we can obtain a strict, distribution-free upper bound by replacing the integrand with its supremum over all possible spatial realizations $\tilde{\mathbf{S}} \in \mathbb{R}^{2T}$. Because this supremum is strictly independent of the interpolation parameter t , the integral trivially evaluates to 1, leaving us with the bound:

$$\mathcal{E}_{\text{measure}} \leq \frac{1}{2} \|\Delta C\|_\infty \sup_{\tilde{\mathbf{S}}} \sum_{i,j,c,e=1}^{2,2,T,T} \left| \frac{\partial^2 f(\tilde{\mathbf{S}})}{\partial \tilde{S}_{(i,c)} \partial \tilde{S}_{(j,e)}} \right|. \quad (24)$$

Next, we bound the L_1 norm (the sum of absolute values) by showing each summand scales as $O(1/T^2)$. To this end, we use the algebraic constraints set on the $A_c(\mathbf{s}_i)$ by the Softmax.

Lemma E.1 (Absolute Hessian Sum of Softmax). *For $A_c = \text{Softmax}(\mathbf{S})_c$, the sum of the absolute values of its first and second derivatives with respect to the logits \mathbf{S} are universally bounded independently of T :*

$$\sum_{k=1}^T \left| \frac{\partial A_c}{\partial S_k} \right| \leq 2A_c, \quad (25)$$

$$\sum_{k,l=1}^T \left| \frac{\partial^2 A_c}{\partial S_k \partial S_l} \right| \leq 6A_c. \quad (26)$$

Proof. The first derivatives are $\partial_k A_c = A_c(\delta_{ck} - A_k)$. Taking the absolute sum:

$$\begin{aligned} \sum_{k=1}^T |A_c(\delta_{ck} - A_k)| &= A_c(1 - A_c) + \sum_{k \neq c} A_c A_k \\ &= 2A_c(1 - A_c) \leq 2A_c. \end{aligned} \quad (27)$$

The second derivatives are derived via the product rule:

$$\begin{aligned} \partial_{kl}^2 A_c &= \frac{\partial}{\partial S_l} (A_c \delta_{ck} - A_c A_k) \\ &= A_c \delta_{ck} \delta_{cl} - A_c A_l \delta_{ck} - A_c A_k \delta_{cl} \\ &\quad - A_c A_k \delta_{kl} + 2A_c A_k A_l. \end{aligned} \quad (28)$$

Applying the triangle inequality and summing over k, l :

$$\begin{aligned} \sum_{k,l=1}^T |\partial_{kl}^2 A_c| &\leq \sum_{k,l=1}^T \left(A_c \delta_{ck} \delta_{cl} + A_c A_l \delta_{ck} \right. \\ &\quad \left. + A_c A_k \delta_{cl} + A_c A_k \delta_{kl} + 2A_c A_k A_l \right). \end{aligned} \quad (29)$$

Using $\sum_{k=1}^T A_k = 1$ and $A_k \geq 0$, the summations directly evaluate to:

$$\begin{aligned} \sum_{k,l=1}^T |\partial_{kl}^2 A_c| &\leq A_c \\ &\quad + A_c(1) + A_c(1) + A_c(1) + 2A_c(1) = 6A_c. \end{aligned} \quad (30)$$

□

We apply Lemma E.1 to our integrand $f(\tilde{\mathbf{S}}) = \sum_{c,e=1}^T A_c(\mathbf{S}^{(1)}) A_e(\mathbf{S}^{(2)}) \Sigma'_{ce}(X_1, X_2)$, and adopt a shorthand notation $A_c(\mathbf{S}^{(1)}) = A_c$ and $A_e(\mathbf{S}^{(2)}) = A_e$. By the product rule, the absolute Hessian over all $2T \times 2T$ variables decomposes into three blocks:

$$\begin{aligned} \sum_{i,j,k,l=1}^{2,2,T,T} \left| \frac{\partial^2 f}{\partial \tilde{S}_{(i,k)} \partial \tilde{S}_{(j,l)}} \right| &= \sum_{k,l=1}^T \left| \frac{\partial^2 f}{\partial S_k^{(1)} \partial S_l^{(1)}} \right| \\ &\quad + \sum_{k,l=1}^T \left| \frac{\partial^2 f}{\partial S_k^{(2)} \partial S_l^{(2)}} \right| + 2 \sum_{k,l=1}^T \left| \frac{\partial^2 f}{\partial S_k^{(1)} \partial S_l^{(2)}} \right|. \end{aligned} \quad (31)$$

We bound each block sequentially. For the first block:

$$\begin{aligned} \sum_{k,l=1}^T \left| \sum_{c,e=1}^T \left(\frac{\partial^2 A_c}{\partial S_k^{(1)} \partial S_l^{(1)}} \right) A_e \Sigma'_{ce} \right| &\leq \sum_{c,e=1}^T (6A_c) A_e \|\Sigma'\|_\infty \\ &\leq 6 \|\Sigma'\|_\infty \leq 6M. \end{aligned} \quad (32)$$

By symmetry, the second block is also bounded by $6M$. For the cross-derivative block:

$$\begin{aligned} \sum_{k,l=1}^T \left| \sum_{c,e=1}^T \left(\frac{\partial A_c}{\partial S_k^{(1)}} \right) \left(\frac{\partial A_e}{\partial S_l^{(2)}} \right) \Sigma'_{ce} \right| &\leq \|\Sigma'\|_\infty \sum_{c,e=1}^T \left(\sum_{k=1}^T \left| \frac{\partial A_c}{\partial S_k^{(1)}} \right| \right) \left(\sum_{l=1}^T \left| \frac{\partial A_e}{\partial S_l^{(2)}} \right| \right) \\ &\leq M \sum_{c,e=1}^T (2A_c)(2A_e) = 4M. \end{aligned} \quad (33)$$

Substituting these into Eq. (31), the absolute Hessian sum of

the entire $2T$ -dimensional integrand is universally bounded:

$$\begin{aligned} \sup_{\tilde{\mathbf{S}}} \sum_{i,j,c,e=1}^{2,2,T,T} \left| \frac{\partial^2 f}{\partial \tilde{S}_{(i,c)} \partial \tilde{S}_{(j,e)}} \right| &\leq 6M + 6M + 2(4M) \\ &= 20M. \end{aligned} \quad (34)$$

Applying this to Eq. (24), the error along the Gaussian measure pathway is bounded by:

$$\begin{aligned} \mathcal{E}_{\text{measure}} &\leq \frac{1}{2} (2M \|\Delta\|_\infty + \|\Delta\|_\infty^2) (20M) \\ &= 20M^2 \|\Delta\|_\infty + 10M \|\Delta\|_\infty^2. \end{aligned} \quad (35)$$

Combining the value and measure error, and taking the leading order term for reasonably bounded estimation errors (assuming $\|\Delta\|_\infty \leq M$), the maximum propagation error through the attention layer is strictly bounded by:

$$\begin{aligned} \|\Delta \Sigma^{\text{next}}\|_\infty &\leq \mathcal{E}_{\text{val}} + \mathcal{E}_{\text{measure}} \\ &\leq (1 + 30M^2) \|\Delta\|_\infty. \end{aligned} \quad (36)$$

The Lipschitz constant of the attention kernel recursion is $\mathcal{L}_{\text{attn}} = 1 + 30M^2$. Because $M = O(1)$, this constant is independent of T .

E.2. Error Propagation in the MLP Layer

As outlined in App. A.3, the propagation through an MLP layer relies strictly on the diagonal elements of the token-to-token matrix. The update rule is element-wise:

$$\Sigma_{ab}^{\text{next}} = \sigma_b^2 + \sigma_W^2 \mathbb{E}_{(z_a, z_b) \sim \mathcal{N}(0, k)} [\phi(z_a) \phi(z_b)]. \quad (37)$$

Here, the Gaussian expectation operates over a bivariate normal distribution parameterized entirely by the 2×2 covariance matrix k , whose elements are comprised of Σ'_{aa} , Σ'_{ab} , and Σ'_{bb} . Because there is no summation or mixing across the T sequence indices, a perturbation $\|\Delta\|_\infty$ in the input covariance matrix merely perturbs the 2×2 matrix k by at most $\|\Delta\|_\infty$.

For standard activation functions bounded by linear growth (e.g., ReLU or GeLU), the dual activation integral is known to be smooth and uniformly Lipschitz continuous with respect to the input covariance entries (Schoenholz et al., 2017). Consequently, the local error simply scales by a bounded, architecture-dependent constant \mathcal{L}_{mlp} such that $\|\Delta \Sigma^{\text{next}}\|_\infty \leq \mathcal{L}_{\text{mlp}} \|\Delta\|_\infty$. This integration acts strictly locally in the sequence dimension and inherently exhibits zero dependence on T .

E.3. Conclusion

Since both the Attention and MLP kernel recursions possess T -independent max-norm Lipschitz bounds, an initial

Monte Carlo error ϵ_0 at the first layer will magnify to at most $\epsilon_L \leq (\mathcal{L}_{\text{attn}}\mathcal{L}_{\text{mlp}})^L \epsilon_0$ after L layers. For a finite-depth network, this is a fixed constant scaling factor.

Consequently, to ensure that the final estimated kernel maintains an absolute approximation error $|f_\delta^{\text{MC}}(X) - f_\delta(X)| < \Delta/6$, the required estimation precision per layer does not depend on the context length T . The necessary number of Monte Carlo samples $N_{\text{MC}} \propto 1/\epsilon_0^2$ therefore remains agnostic of T .